Study of the red blood cell aggregation by coherent anti-Stokes Raman spectroscopy

Martín A. Toderi[a,b], Gustavo E. Galizzi[a,c], Bibiana D. Riquelme[a,b], and Dominique Dumas[d]

[a]Instituto de Física Rosario (CONICET-UNR), Bv. 27 de Febrero 210 bis, Rosario, Argentina.
[b]Facultad de Cs. Bioquímicas y Farmacéuticas - Universidad Nacional de Rosario, Suipacha 531, Rosario, Argentina.
[c]Facultad de Cs. Exactas, Ingeniaría y Agrimensura - Universidad Nacional de Rosario, Pellegrini 250, Rosario, Argentina.
[d]UMS2008 IBSLor-Ingénierie Moléculaire et Physiopathologie Articulaire UMR 7365 CNRS-Université de Lorraine CNRS-UL-INSERM. 9 Avenue de la Forêt de Haye, Vandœuvre-lès-Nancy, France.

ABSTRACT

In this work, we studied the nature of the molecular bonds involved in the red blood cell aggregation process by the coherent anti-Stokes Raman spectroscopy technique. Images were acquired with a commercial Leica TCS SP8 CARS confocal microscope (Leica Microsystems GmbH, Wetzlar, Germany) temporally and spatially overlapping the pulses of two sources in the focal plane of the microscope. A pump wavelength of 810 nm to 817 nm was used for the CARS mode simultaneously with the Stokes beam at 1064 nm to excite the vibratory resonance of the symmetric hydrocarbon bonds in the lipids and that of the bonds in amino acids of the proteins. The Raman shift was also observed at the 1200 cm^{-1} range to study possible variations in the sialic acid on the cell membrane produced by concentrations of dextran 500 in the suspension medium. Curves of lifetime emission distribution were obtained for untreated erythrocytes and treated erythrocytes with dextran 500, particularly at a pump wavelength of 904 nm.

Keywords: erythrocyte aggregation, coherent anti-Stokes Raman spectroscopy, dextran

1. INTRODUCTION

The study of blood dynamics is an element of interest in the field of biomedicine. The study of the erythrocyte morphology, interaction and dynamics is essential for the diagnosis of several pathologies and anomalies that can alter the microcirculation disturbing the well functioning of the organism. Hemorheological studies are a useful tool for the detection and quantification of alterations in various pathologies, such as diabetes, high blood pressure and anemias. These investigations also allow the analysis of the hemorheological action of various agents (medications, anesthetics, biomaterials, etc.)[1–3] Imaging methods by bright-field microscopy, optical techniques such as light scattering, light transmission and laser biospeckle[4–6] allow to obtain characteristic parameters at different states of the dynamics of blood components. These methods rely on the collective behavior of the red blood cells (RBC) and are suitable for clinical determinations but they do not directly inquire about the specific alterations in the cell membrane order. In this work we observed the RBC individually and in individual cell assemblies of few RBC.

Further author information: (Send correspondence to Martín A. Toderi)
E-mail: toderi@ifir-conicet.gov.ar

1.1 RBC aggregation

Blood viscosity is determined by plasma viscosity and RBCs concentration (hematocrit), deformation, and aggregation.[7] The extreme deformability of the RBC is very important in the microcirculation as they have a larger diameter than microvessels. The fluidity of blood is due directly to the viscoelastic properties of the erythrocytes,[8] favored by a loose membrane that gives them a high surface/volume ratio. Erythrocytes tend to form aggregates that initially consist of face to face linear structures resembling a stack of coins which are generally called "rouleaux"[9] (see Fig. 1). The greater or lesser tendency to aggregate will depend on a balance of the factors that favor or hinder RBC aggregation. Among the aggregation inhibitors are: the electrostatic repulsion of the RBCs caused by the negative electric charge of the erythrocyte surface; the elasticity of the membrane, since aggregation implies a certain degree of erythrocyte deformation; and in flow regime, the existence of shear stresses due to the flow velocity that tends to separate RBCs aggregates. On the other hand, the factors that promote aggregation are low or zero shear stress, the presence of macromolecules in the suspension medium (in particular fibrinogen) and intrinsic factors of the erythrocytes.[10] Interactions between RBCs that lead to the formation of erythrocyte aggregates or anomalous "clusters" that are excessively resistant to dissociation have been frequently observed in pathological situations such as diabetes and hypertension.[11] Several techniques have been developed to analyze the adhesion of erythrocytes by optical methods.[12–14] Dynamic techniques are particularly important because they provide information on the interaction between the macromolecules involved in this phenomenon.[15]

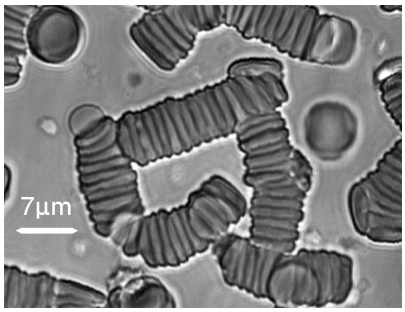

Figure 1. Image of typical rouleaux structures for RBCs under no shear stresses and suspended in autologous plasma. The photo was taken with a 40X objective and a confocal microscope in bright field mode.

1.2 Dextran as a RBC aggregation promoter

Dextran is a complex and branched polysaccharide formed by numerous glucose molecules, forming units in chains of variable weights (40, 70, 500 kDa). Dextran of different molecular mass present different levels of effectiveness in erythrocyte aggregate formation.[16] The macromolecules adhesion to the erythrocyte surface provides binding sites giving place to the combined phenomena of depletion and bridging.[17,18] We used dextran 500 kDa as studies indicated that it is the optimal for inducing the aggregation phenomenon.[16] Dextran, unlike fibrinogen, causes RBCs to aggregate until a maximum concentration beyond which the formation of structures is prevented.

1.3 Coherent anti-Stokes Raman spectroscopy

Spontaneous Raman scattering (SRS) and infrared imaging are common methods in vibrational microscopy. Infrared is limited by low spatial resolution because of the large wavelengths involved. As SRS microscopy works in the visible or near-infrared wavelengths it avoids this problem, however, it is limited by its low cross section. Coherent anti-Stokes Raman spectroscopy (CARS) presents a signal that is consequence of a collective vibrational oscillation with a well defined phase and its intensity grows quadratically with the number of molecules. Photons are emitted in the direction where the signal is constructive, this condition is known as phase-matching.[19] The studied sample is illuminated simultaneously with a pump frequency and a Stokes frequency, being the difference between them the resonant vibrational frequency of the excited molecular bond,[20] $\Omega_R = \omega_P - \omega_S$, as depicted in Fig. 2. Photons of other frequencies can constitute electronic noise and non resonant contributions. CARS

results in a useful technique for noninvasive studies in biological elements as it prevents photochemical damage, it has chemical selectivity and 3D sectioning capability, and more importantly it does not require to use dyers as contrast mechanism.

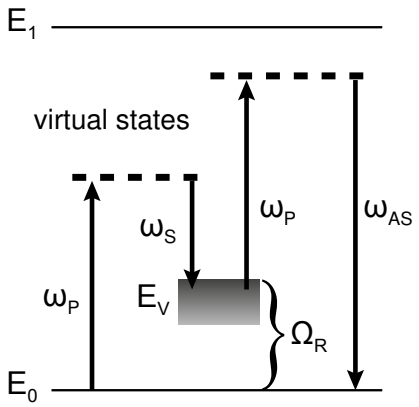

Figure 2. Energy diagram for the CARS process. The anti-Stokes emission (ω_{AS}) is generated through the combination of both the pump (ω_P) and Stokes (ω_S) beams. Starting from the ground state E_0 the electronic excited state E_1 is never reached. E_V is the vibrational state of the resonant Raman mode.

2. MATERIALS AND METHODS

Two stages can be distinguished, sample preparation and the application of the CARS technique. All experiments were conducted within 24 hours of the blood extraction following the recommendations of Ref. 21.

2.1 Blood Sample Preparation

Whole blood samples were obtained from consented healthy donors by venous puncture and anticoagulated with EDTA. Donors did not have any pre-existing health problems (e.g. cardiovascular disease, respiratory disease, endocrine disease, hematological disorders or neoplasm etc.) and had normal hepatic, and renal function, coagulation and complete blood count. RBCs were obtained from whole blood centrifuged for 5 minutes at 2000 rpm (Paralwall Model PWL 12T). Buffy coat was discarded and plasma was separated and reserved for further use. RBCs were washed two times with phosphate buffered saline (PBS).

2.1.1 Dextran and suspension medium

A suspension medium (SM) to replace autologous plasma was prepared mixing PBS, EDTA (0.056%) and albumin (BSA Sigma) at 0.5%. In particular, albumin is vital to prevent glass effect on the RBCs and to keep the integrity of the cells. To induce the formation of erythrocyte aggregates, dextran 500 (i.e. 500 kDa of molecular weight) was used. A main solution of dextran at 10% in PBS was prepared and mixed with the SM to constitute solutions of dextran at 0.6 and 0.8 g/dL. Afterward, suspensions of RBCs in these dextran mediums were prepared along with a control with no dextran. Additionally, a preparation with autologous plasma was made. All samples had a fixed concentration of 2% of RBCs in the solution volume suitable for microscopy imaging.

2.2 Experimental setup

The images were acquired with a commercial Leica TCS SP8 CARS confocal microscope (Leica Microsystems GmbH, Wetzlar, Germany), which consisted of an inverted microscope equipped with an ultra-short pulsed light source (picoEmerald, APE, Berlin, Germany) that produces the two synchronous beams needed for CARS (Fig. 3). The Stokes beam at 1064 nm was emitted from a neodymium-doped yttrium orthovanadate ($Nd:YVO_4$) laser while a tunable pump/probe beam at 780–943 nm was generated by an optical parametric oscillator (OPO). The pulse width was 5–7 ps with a repetition rate of 80 MHz corresponding to the Raman line width of 2 to 3 cm^{-1}. The pulses from the two sources were temporally and spatially overlapped on the focal plane of the microscope

as shown in Fig. 3. Up to 100 mW of average power from both the pump and the Stokes source was delivered to the RBCs with an identical laser intensity for each measurement. The laser generating wavelength of 817 nm was used for the CARS modality simultaneously with the Stokes beam at 1064 nm to excite the symmetric vibrational resonance of the CH_2 hydro-carbon bonds in the membrane lipids at 2845 cm^{-1} and that of the CH_3 bonds in amino acids of the proteins. Likewise, the 1200 cm^{-1} range was observed with pump wavelengths of 880-940 nm. The coherent anti-Stokes Raman scattering signal was detected in the epi-direction using a non-descanned photomultiplier tube (Hybrid-PMT) detector.

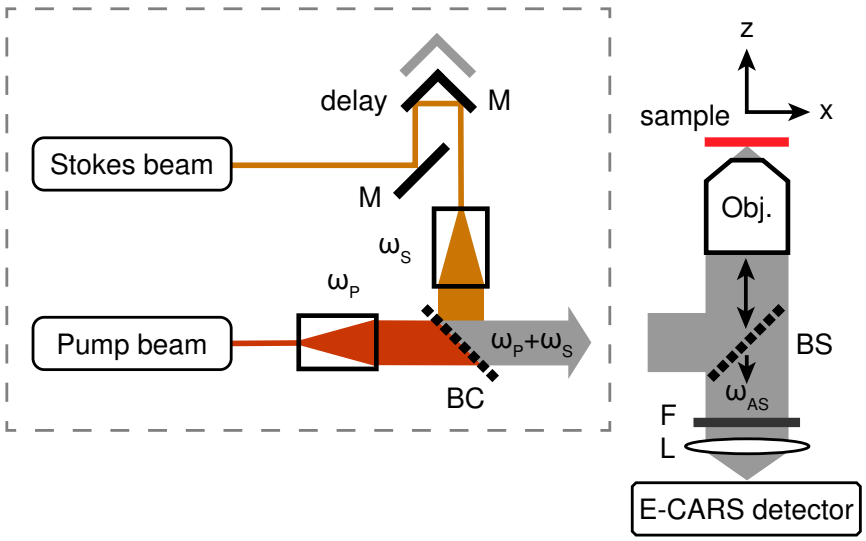

Figure 3. Scheme of the Epi-CARS setup with co-propagating incident beams, pump (ω_P) and Stokes (ω_S). ω_{AS} is the anti-Stokes emission; M, mirror; Obj., objective lens; F, filter; BS, beam splitter; BC, beam combiner; L, lens and M., mirror.

3. RESULTS AND DISCUSSION

The action of dextran produced different morphologies on the erythrocyte aggregates. Longer and more complex aggregate networks are present when dextran interacts with the cell membrane as shown in Fig. 4.

Firstly, an intensity profile was calculated in order to establish baseline conditions. Figure 5 (a) depicts the mean intensity in the cell region and in the background for a wavelength sweep between 794 and 810 nm of a sample of RBC with plasma. Low contrast conditions can be noticed due to the components of the plasma resulting in a high background signal. This is one of the main reasons why a SM with albumin was used. The intensity profile was also studied for isolated RBCs, dextran-treated RBCs and aggregates showing better contrast conditions, in particular for the 1200 cm^{-1} range as seen in Fig. 5 (b).

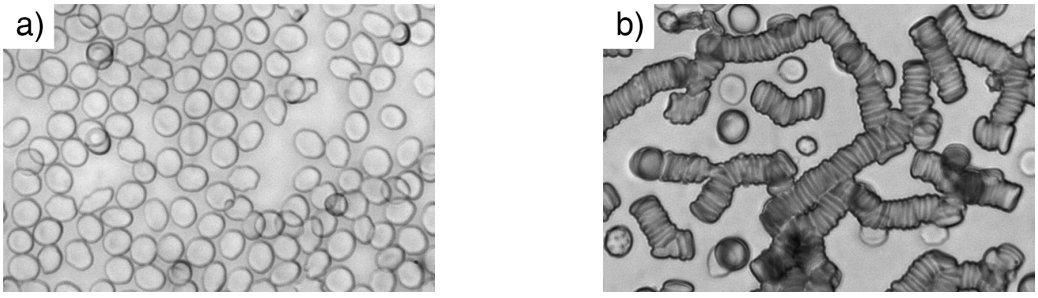

Figure 4. Red blood cells suspended in PBS with albumin (a) and mixed with dextran medium at 0.8 g/dL (b).

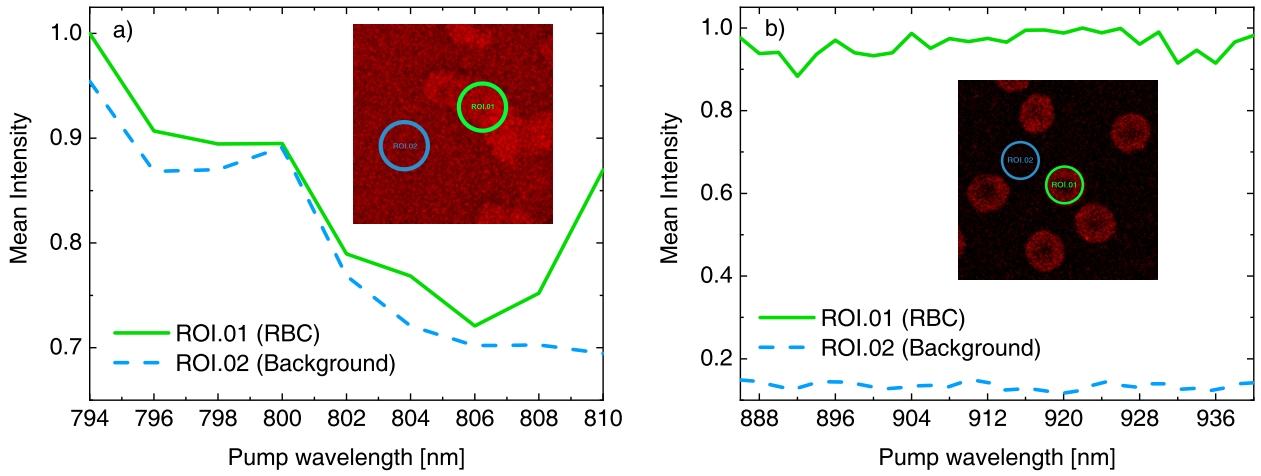

Figure 5. Intensity profiles of RBCs suspended in plasma for a pump wavelength of 794-810 nm (a) and suspended in PBS with albumin for a pump wavelength of 886-940 nm (b).

Figure 6 shows images of cells for Raman shifts of 2845 cm^{-1} and 1460 cm^{-1}. Different details are observed for the same echinocyte (Fig. 6 (a) and (b)). An echinocyte is an abnormal RBC that has evenly spaced thorny projections through the membrane. Measurements imply a redistribution of the protein lipids and amino acids around the spicular structures. In Fig. 6 (c), a few RBCs aggregate formed in dextran 0.6 g/dL solution presents higher intensity in the external faces where the binding sites in the membrane are not fully filled.

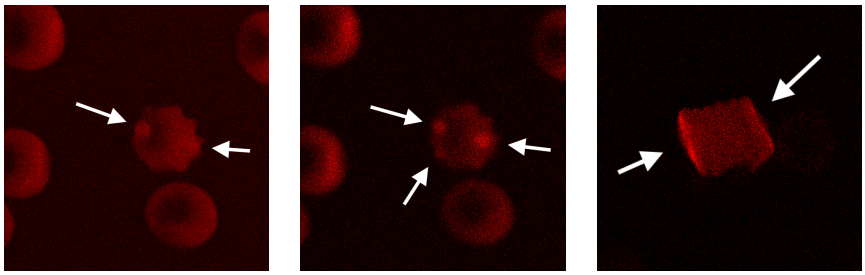

(a) (b) (c)

Figure 6. Images of an echinocyte illuminated with a pump wavelength of 817 nm (a) and a pump wavelength of 921 nm (b). Small rouleaux in solution of dextran at 0.6 g/dL for a pump wavelength of 817 nm (c).

To analyze the cell morphology under different suspension medium conditions, a line profile of the intensity was calculated. This would approach a cross-section of the cell. The typical biconcave shape of the RBCs is altered by dextran as seen in Fig. 7. This could be attributed to a rearrangement of the membrane structures and therefore variations of the stretching/shear elastic energies of the membrane skeleton.

A system capable of measuring the lifetime emission of the collected signals was applied for further analysis. Typically, a coherent anti-Stokes Raman scattering profile corresponds to emission lifetimes less than 0.4 ns. In fluorescence microscopy this analysis is known as florescence lifetime imaging (FLIM). The fluorescence lifetime is defined as the time the emitter remains in the excited state before returning to the ground state. Time-correlated single photon counting (TCSPC) measures the time between sample excitation and the arrival of the emitted photon at the detector. The lifetime emission profile of two samples is shown in Fig. 8. It can be noticed a strong peak of 0.2-0.3 ns wide and some fluorescence decay mixed in the process. This analysis is intended to register the actual presence of the coherent emission phenomenon.

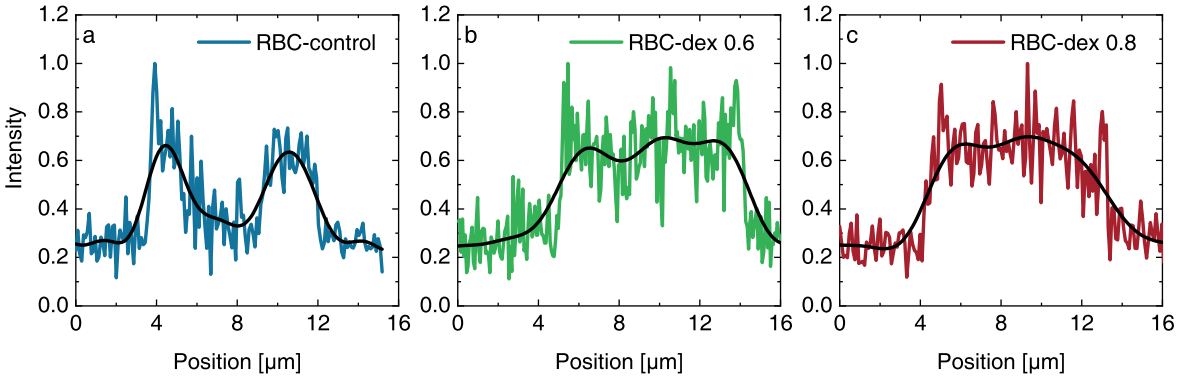

Figure 7. Line profiles at a pump wavelength of 817 nm for a single RBC suspended in SM (a) dextran 0.6 g/dL solution (b) and dextran 0.8 g/dL (c).

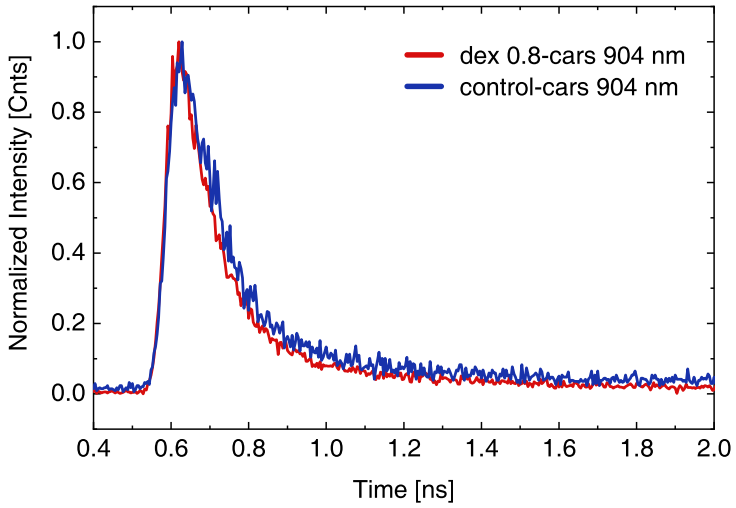

Figure 8. Fluorescence lifetime emission distributions for single control RBCs and rouleaux due to dextran at 0.8 g/dL concentration. Pump wavelength was 904 nm corresponding to a 1660 cm^{-1} Raman shift.

4. CONCLUSIONS

In this work we addressed possible changes in the membrane structure of the RBCs by CARS, in particular those related to RBC adhesion. The effect of a well known polysaccharide such as dextran was observed and new guidelines could arise from further studies. The RBC aggregation process is not fully elucidated, and the application of new light-based and label-free technologies such as CARS to the study of blood will propose novel approaches. Analyzing the RBCs response to different environments and characterizing the adhesion phenomenon, will contribute to the development of tools for diagnosis and treatment of vascular pathologies, where microcirculation plays a fundamental role.

ACKNOWLEDGMENTS

Authors want to acknowledge the financial support from CPER IT2MP_IMTI_A1_25 France – FEDER Union Européenne – Region Grand EST. First author wants to thank the PTIBC - IMoPA - UL platform and specially Dr. Dominique Dumas for his guidance and mentorship.

REFERENCES

[1] Riquelme, B. D., Foresto, P., D'Arrigo, M., and Rasia, R. J., "Laser diffractometry technique for determination of stationary and dynamics viscoelastic parameters of erythrocyte in vascular pathologies," in [*Optical Coherence Tomography and Coherence Techniques*], Drexler, W., ed., **5140**, 229 – 237, International Society for Optics and Photonics, SPIE (2003).

[2] Ponce de Leon, P., Toderi, M., Castellini, H., and Riquelme, B., "In vitro alterations of erythrocyte aggregation by action of trichinella spiralis newborn larvae," *Clinical Hemorheology and Microcirculation* **65**(2), 195–204 (2017).

[3] Alet, A. I., Basso, S., Delannoy, M., Alet, N. A., D'Arrigo, M., Castellini, H. V., and Riquelme, B. D., "Innovative parameters obtained for digital analysis of microscopic images to evaluate in vitro hemorheological action of anesthetics," in [*Biophotonics South America*], D.D.S., C. K., M.D., K. S., Tromberg, B. J., and Bagnato, V. S., eds., **9531**, 187 – 192, International Society for Optics and Photonics, SPIE (2015).

[4] Riquelme, B. D., Valverde, J. R., and Rasia, R. J., "Determination of the complex viscoelastic parameters of human red blood cells by laser diffractometry," in [*Optical Diagnostics of Biological Fluids V*], Priezzhev, A. V. and Asakura, T., eds., **3923**, 132 – 140, International Society for Optics and Photonics, SPIE (2000).

[5] Toderi, M. A., Castellini, H. V., and Riquelme, B. D., "Descriptive parameters of the erythrocyte aggregation phenomenon using a laser transmission optical chip," *Journal of Biomedical Optics* **22**(1), 1 – 8 (2017).

[6] Toderi, M. A., Riquelme, B. D., and Galizzi, G. E., "An experimental approach to study the red blood cell dynamics in a capillary tube by biospeckle laser," *Optics and Lasers in Engineering* **127**, 105943 (2020).

[7] Popel, A. S. and Johnson, P. C., "Microcirculation and hemorheology," *Annual Review of Fluid Mechanics* **37**(1), 43–69 (2005).

[8] Riquelme, B., Castellini, H., and Albea, B., "Linear and non-linear viscoelasticity of red blood cells using a new optical erythrocyte rheometer," in [*Latin America Optics and Photonics Conference*], *Latin America Optics and Photonics Conference* , Th4A.41, Optical Society of America (2018).

[9] Chien, S. and Sung, L. A., "Physicochemical basis and clinical implications of red cell aggregation," *Clinical Hemorheology* **7**, 71–91 (1987).

[10] Fåhræus, R. and Lindqvist, T., "The viscosity of the blood in narrow capillary tubes," *American Journal of Physiology-Legacy Content* **96**(3), 562–568 (1931).

[11] Delannoy, M., Fontana, A., D'arrigo, M., and Riquelme, B. D., "Influence of hypertension and diabetes on erythrocyte aggregation using image digital analysis," *Series on Biomechanics* **29**(1), 5 – 10 (2015).

[12] Riquelme, B. D., Dumas, D., de Rasia, J. V., Rasia, R. J., and Stoltz, J. F., "Analysis of the 3D structure og agglutinated erythrocyte using CellScan and confocal microscopy: characterization by FLIM-FRET," in [*Confocal, Multiphoton, and Nonlinear Microscopic Imaging*], Wilson, T., ed., **5139**, 190 – 198, International Society for Optics and Photonics, SPIE (2003).

[13] Fontana, A.and Lerda, N., Delannoy, M., Alessi, A., and Riquelme, B., "Erythrocyte aggregation quantification technique using digital image analysis," *Acta Bioquímica Clínica Latinoamericana* **46**(1), 47–52 (2012).

[14] Riquelme, B. D. and Londero, C. M., "New optical approach to simultaneous determination of deformability and adhesion energy of human erythrocytes," in [*Latin America Optics and Photonics Conference*], *Latin America Optics and Photonics Conference* , Th4A.39, Optical Society of America (2018).

[15] Dumas, D., Gaborit, N., Grossin, L., Riquelme, B., Gigant-Huselstein, C., De Isla, N., Gillet, P., Netter, P., and Stoltz, J., "Spectral and lifetime fluorescense imaging microscopies: New modalities of multiphoton microscopy applied o tissue or cell engineering," *Biorheology* **41**(3), 459–467 (2004).

[16] Neu, B., Wenby, R., and Meiselman, H. J., "Effects of dextran molecular weight on red blood cell aggregation," *Biophysical Journal* **95**(6), 3059 – 3065 (2008).

[17] Fantoni, R., Giacometti, A., and Santos, A., "Bridging and depletion mechanisms in colloid-colloid effective interactions: A reentrant phase diagram?," *The Journal of Chemical Physics* **142**, 224905 (03 2015).

[18] Lee, K., Shirshin, E., Rovnyagina, N., Yaya, F., Boujja, Z., Priezzhev, A., and Wagner, C., "Dextran adsorption onto red blood cells revisited: single cell quantification by laser tweezers combined with microfluidics," *Biomed. Opt. Express* **9**, 2755–2764 (Jun 2018).

[19] Zumbusch, A., Holtom, G. R., and Xie, X. S., "Three-dimensional vibrational imaging by coherent anti-stokes raman scattering," *Phys. Rev. Lett.* **82**, 4142–4145 (May 1999).

[20] Potma, E. O., Jones, D. J., Cheng, J.-X., Xie, X. S., and Ye, J., "High-sensitivity coherent anti-stokes raman scattering microscopy with two tightly synchronized picosecond lasers," *Opt. Lett.* **27**, 1168–1170 (Jul 2002).

[21] Baskurt, O. K., Boynard, M., Cokelet, G. C., Connes, P., Cooke, B. M., Forconi, S., Liao, F., Hardeman, M. R., Jung, F., Meiselman, H. J., Nash, G., Nemeth, N., Neu, B., Sandhagen, B., Shin, S., Thurston, G., and Wautier, J. L., "New guidelines for hemorheological laboratory techniques," *Clinical Hemorheology and Microcirculation* **42**(2), 75–97 (2009).